Elastomeric Poly(propylene): Propagation Models and Relationship to Catalyst Structure

William J. Gauthier[1] and Scott Collins*

Department of Chemistry, University of Waterloo, Waterloo, Ontario, Canada N2L 3G1

Received November 1, 1994; Revised Manuscript Received March 2, 1995[⊗]

ABSTRACT: Propylene polymerizations were conducted with a number of chiral metallocene complexes of titanium, zirconium, and hafnium, and the polymers were characterized by ^{13}C NMR spectroscopy. In certain cases, elastomeric material is produced. The microstructure of the polymers prepared, as determined by ^{13}C NMR spectroscopy, has been simulated using several statistical models for propagation. The models are formulated in terms of different mechanisms for monomer insertion at the two, inequivalent coordination sites in this family of catalysts. This work has revealed that the microstructure of this polymer can be adequately described by more than one model and that a range of acceptable parameters exists for each of these models. Arguments are presented that the microstructure of elastomeric poly(propylene) is much more random than originally proposed and that if blocks of e.g., atactic sequences are present, they are, on average, very short.

Introduction

Analysis of polyolefin structure by ^{13}C NMR spectroscopy has led to major advances in our understanding of the propagation and chain transfer processes involved in olefin polymerization using both conventional Ziegler–Natta and single-site metallocene complexes. In particular, the study of stereoregular polymers derived from α-olefins such as propylene has been particularly informative; models for the stereochemical microstructure of such polymers have been derived, based on fundamental propagation statistics, that can be directly tested by comparison to experimentally observed, stereochemical distributions.[2]

Recently, a catalyst system derived from titanocene complex **1** (Scheme 1) and methylaluminoxane (MAO) has been used to polymerize propylene and, depending on polymerization conditions, produces PP with elastomeric properties.[3]

As outlined in the previous paper,[4] structurally related catalysts such as **2**–**6** (Scheme 1) can also provide this material, provided that high molecular weight polymer (M_w > 50K) with low stereoregularity (i.e., % mmmm ~40–50%) can be prepared.

The mechanism that has been invoked to account for the presence[5] of crystallizable and amorphous segments in PP prepared using catalyst **1** is patterned after a two-state model for propagation originally described by Coleman and Fox.[6]

In this version of the two-state model (Scheme 1), the formation of crystalline domains involves consecutive insertions from one of the lateral coordination sites (site 1) of catalyst **1** so as to give rise to isotactic sequences, whereas consecutive insertions at the other site (site 2) should give rise to atactic, amorphous sequences. Interconversion between these two states must occur within the lifetime of a given polymer chain in order to generate a physically cross-linked network and is believed to occur via isomerizations of the polymer chain. Thus, the microstructure of elastomeric poly(propylene) (elPP) produced using catalyst **1** is considered to be built up of blocks of atactic and isotactic sequences, with the latter being of sufficient length to cocrystallize with similar sequences on other polymer chains.

Scheme 1

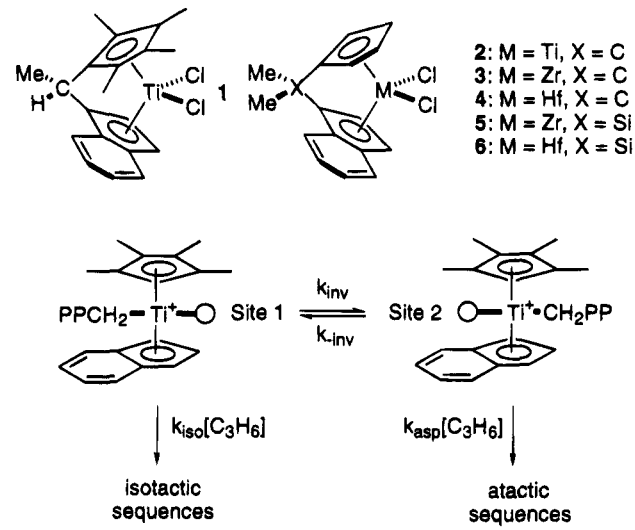

The microstructure of elPP, as determined by ^{13}C NMR spectroscopy at the pentad level, has been successfully described using this consecutive two-state model for propagation.[7] Based on the physical (i.e., elastomeric) properties of elPP, the average sequence lengths of amorphous domains were derived[5] and were used as initial (and partially constrained) parameters in the simulation.

Although the pentad intensities could be satisfactorily reproduced using such a model, one may question whether the assumption of "fixed" sequence lengths is justifiable or even whether this model uniquely describes the microstructure of elPP at some arbitrary level of accuracy consistent with the experimental data.

There are compelling fundamental reasons for raising these questions. In particular, the mechanism for olefin insertion in these polymerizations involves a classical, migratory insertion reaction in which the growing polymer chain migrates to the β-carbon of the coordinated olefin (Scheme 2). Thus, the insertion process results in migration of the chain to the lateral site formerly occupied by coordinated monomer. In order for further insertion to occur from this site, as required by a consecutive two-state model, the chain must migrate to its previous location, a process that formally involves inversion at the metal center.

[⊗] Abstract published in *Advance ACS Abstracts,* April 15, 1995.

0024-9297/95/2228-3779$09.00/0

Scheme 2

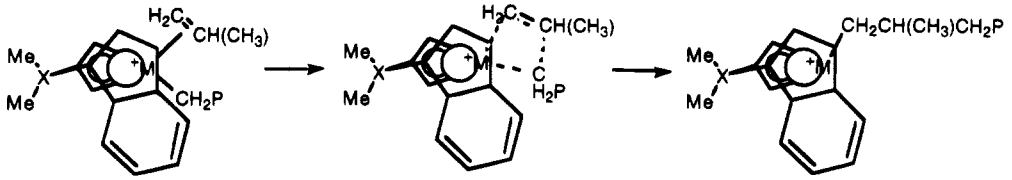

Table 1. Normalized Pentad Intensities for Poly(propylene) Produced Using Catalysts 2–6

		pentad								
cat.	conditions[a]	mmmm	mmmr	rmmr	mmrr	mmrm + rmrr	mrmr	rrrr	mrrr	mrrm
2	25 (15)	0.359	0.175	0.026	0.149	0.111	0.043	0.016	0.050	0.070
4	25 (15)[b]	0.373	0.182	0.030	0.188	0.066	0.016	0.019	0.035	0.091
4	25 (45)	0.315	0.181	0.031	0.198	0.077	0.020	0.036	0.054	0.089
4	0 (15)	0.385	0.168	0.030	0.185	0.059	0.019	0.024	0.037	0.094
5	25 (15)[c]	0.298	0.174	0.043	0.156	0.116	0.058	0.025	0.048	0.084
6	25 (15)[c]	0.534	0.159	0.020	0.140	0.042	0.021	0.009	0.014	0.067
6	25 (60)	0.496	0.160	0.033	0.134	0.056	0.030	0.009	0.020	0.062
6	0 (45)	0.522	0.152	0.043	0.133	0.051	0.023	0.020	0.019	0.054

[a] Temperature of polymerization (°C) with propylene pressure (psig) in parentheses. [b] Average of three different polymer samples prepared under the same conditions; the standard deviation is ±5%. [c] Average of two different polymer samples prepared under the same conditions.

Structure I

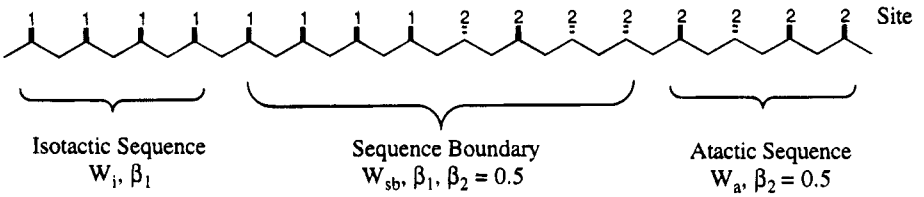

It seemed counterintuitive to us to invoke a consecutive two-state model on this basis. As originally described, only occasional isomerizations (i.e., inversions at the metal center) between the two states were invoked to account for the structure of elPP[3] and yet a consideration of the fundamental processes involved indicates that this same isomerization process must generally occur following *each* insertion in order to generate atactic and isotactic sequences!

In this paper, we present three limiting models for propagation involving catalysts such as **2**–**6** and derive the statistical expressions for the pentad distributions of poly(propylene) for each. No assumptions concerning sequence lengths etc. have been made other than they are at least four monomer units long.[8] The models are critically compared to experimental data on elPP, and the parameter estimates are discussed with reference to other catalytic systems that have been studied.

Results and Discussion

The experimental pentad distributions of a number of poly(propylene) samples prepared using catalysts **2** and **4**–**6** were measured by ^{13}C NMR spectroscopy at 120 °C in 1,2,4-trichlorobenzene solution using inverse-gated decoupling to minimize differential NOE effects. The chemical shift assignments have been reported elsewhere.[9] These data are summarized in Table 1.

Based on the triad test statistic 2(rr)/(mr) = 1, all of the polymer samples examined have microstructures consistent with a site-control model for propagation.[2b] Thus, it seems effects due to chain-end control[2e] can be safely neglected for present purposes.

Model Descriptions. With reference to both Schemes 1 and 2, it is readily apparent that three limiting models for propagation can be developed.

One of these is patterned after the block type structure proposed for elPP and will be referred to as the block model (model I). In this model, the polymer is built up of isotactic and atactic sequences as idealized by structure I.

The isotactic sequences are generated by consecutive insertions at site 1 (Scheme 1) which possesses a characteristic probability for isotactic placements of β_1 whereas the atactic sequences are generated by consecutive insertions at site 2 where insertion was assumed to be stereorandom (i.e., $\beta_2 = 0.5$) but would follow a site-control mechanism. This model was chosen over, e.g., an alternative one developed by Chujo et al.[2e] (which invokes chain-end control at aspecific sites) as the triad distributions obeyed site-control statistics and further, it was not obvious that insertion at the aspecific site would be completely stereorandom (i.e., $\beta_2 \neq 0.5$; vide infra).

For the purposes of the derivation, the polymer structure can be defined in terms of the weight fractions of each of these sequences, W_i and W_a, respectively but also in terms of a sequence boundary (W_{sb}) that, at the pentad level of resolution, is uniquely defined by an eight-monomer sequence that bridges the former two regions of the polymer (structure I). Thus, with this model, there are three independent parameters, β_1, W_i, and W_{sb}, with $W_a = 1 - (W_i + W_{sb})$. It is important to emphasize that, in this model, W_i and W_a are the weight fractions of sequences of five or monomer units arising from insertions at sites 1 and 2, respectively. Thus, these parameters are not directly related to, e.g., the weight fraction of all insertions at a given site and cannot be directly compared to parameters obtained from the other models examined (vide infra).

In the second model, which will be referred to as the random model (model II), the polymer structure is not

considered to be blocky in the sense defined above. Insertions can occur competitively at either site with insertions at site 1 being isospecific (with probability β_1) and those at site 2 being aspecific ($\beta_2 = 0.5$). The frequency of insertion at site 1 is reflected in the bulk, weight fraction parameter W_i whereas insertions at site 2 are defined by W_a, which are different from those parameters developed for the block model. Thus, this model has only two independent parameters (β_1 and W_i).

It should be pointed out that it is still possible to generate isotactic sequences with the random model. For example, such sequences could be built up by consecutive insertions at site 1 (as above) or by a combination of insertions at both sites with the proper relative stereochemistry. The frequency and length of such sequences would however be dictated by simple statistics based on the stereoselectivity of insertion at site 1 and the reactivity differences between the two sites (related to W_i and W_a).

The final model to be considered is one that is closely related to the processes outlined in Scheme 2. One invokes strict alternating insertions at the two sites with the stereoselectivity of insertion at each site as defined above. From a mechanistic viewpoint, chain isomerization is slow relative to the rate of insertion at either site.

If the stereoselectivity of insertion at site 1 is essentially complete ($\beta_1 = 1$) and that at site 2 is perfectly random ($\beta_2 = 0.5$), this model describes the microstructure of hemiisotactic poly(propylene)[10] in which every other insertion is stereoselective. This model will be referred to as the alternate model (model III), and if perfect alternation is assumed, it is only, at most, a two-parameter model with parameters β_1 and β_2. For the purposes of derivation, we will assume that $\beta_2 = 0.5$.

Derivation of the Pentad Intensities. For a given pentad resonance, the normalized intensity can be expressed in terms of the parameters defined for each model. The derivation is tedious and algebraically complex for some of these models and only a single example will be given for each.

For the block model, the pentad intensities for the isotactic and atactic sequences in terms of β_1 and β_2, assuming enantiomorphic site control for consecutive insertions at each site, have been previously derived.[2b] What remains is to derive appropriate expressions for pentads located within the sequence boundary as defined above (structure I). The overall pentad intensity will then be given by the weighted sum of these three contributions where $f(\beta_1)$, $g(\beta_2)$, and $h(\beta_1,\beta_2)$ are functions describing the pentad intensities within each region of the polymer.

$$\text{observed pentad} = W_i f(\beta_1) + W_a g(\beta_2) + W_{sb} h(\beta_1,\beta_2)$$

As shown in Scheme 3, using the block model there are eight possible sequences for, e.g., a mrrr pentad that can be generated by consecutive insertion processes at the two sites. The probability of each sequence, in terms of β_1 and β_2 (=0.5) can be written down by inspection, keeping in mind that the mirror image of the mrrr pentad depicted in Scheme 3 cannot be distinguished by NMR and must thus be counted. The total pentad intensity is the weighted sum of each possible sequence, so a normalization constant of 1/8 = 0.125 is required. Finally, in this particular case, the pentad is unsymmetrical and there are thus two possible arrangements (i.e., order of monomer units) than cannot be distinguished by ^{13}C NMR spectroscopy. The complete expressions for the (normalized) pentad intensities arising from within the sequence boundary are summarized in Table 2 and were derived in a similar manner.

Scheme 3

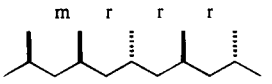

Site of Insertion					Probability of mrrr Pentad	
1	1	1	1	2	$\beta^3(1-\beta)0.5$	$\beta(1-\beta)^3 0.5$
1	1	1	2	2	$\beta^2(1-\beta)0.5^2$	$\beta(1-\beta)^2 0.5^2$
1	1	2	2	2	$\beta^2 0.5^3$	$(1-\beta)^2 0.5^3$
1	2	2	2	2	$\beta 0.5^4$	$(1-\beta)0.5^4$
2	2	2	2	1	$(1-\beta)0.5^4$	$\beta 0.5^4$
2	2	2	1	1	$\beta(1-\beta)0.5^3$	$\beta(1-\beta)0.5^3$
2	2	1	1	1	$\beta(1-\beta)^2 0.5^2$	$\beta^2(1-\beta)0.5^2$
2	1	1	1	1	$\beta^2(1-\beta)^2 0.5$	$\beta^2(1-\beta)^2 0.5$

mrrr = [normalization constant][symmetry factor][sum of probabilities]

mrrr = [0.125][2][sum of probabilities]

$$\text{mrrr} = 0.125\,[\,\beta^3(1-\beta) + \beta(1-\beta)^3 + 2\beta^2(1-\beta)^2 + \beta^2(1-\beta) + \beta(1-\beta)^2\,] + 0.03125\,[\,\beta^2 + (1-\beta)^2 + 2\beta(1-\beta) + 1\,]$$

Table 2. Normalized Pentad Intensities for the Sequence Boundary Using the Block Model[a]

pentad	probability
mmmm	$0.03125\{4[\beta_1^4 + (1-\beta_1)^4] + 2[\beta_1^3 + (1-\beta_1)^3] + [\beta_1^2 + (1-\beta_1)^2 + 0.50]\}$
mmmr	$0.03125\{4[\beta_1^4 + (1-\beta_1)^4 + \beta_1^3(1-\beta_1) + \beta_1(1-\beta_1)^3] + 2[\beta_1^3 + (1-\beta_1)^3 + \beta_1^2(1-\beta_1) + \beta_1(1-\beta_1)^2] + [\beta_1^2 + (1-\beta_1)^2 + 2\beta_1(1-\beta_1) + 1]\}$
rmmr	$0.0625\{2[\beta_1^3(1-\beta_1) + \beta_1(1-\beta_1)^3] + [\beta_1^2(1-\beta_1) + \beta_1(1-\beta_1)^2 + \beta_1(1-\beta_1) + 0.25]\}$
mmrr	$0.0625\{4[\beta_1^3(1-\beta_1) + \beta_1(1-\beta_1)^3] + [\beta_1^3 + (1-\beta_1)^3 + \beta_1^2(1-\beta_1) + \beta_1(1-\beta_1)^2 + \beta_1(1-\beta_1) + 1]\}$
mmrm + rmrr	$0.0625\{2[2\beta_1^3(1-\beta_1) + 2\beta_1(1-\beta_1)^3 + 4\beta_1^2(1-\beta_1)^2 + \beta_1(1-\beta_1)] + [\beta_1^3 + (1-\beta_1)^3 + 3\beta_1^2(1-\beta_1) + 3\beta_1(1-\beta_1)^2 + \beta_1^2 + (1-\beta_1)^2 + 0.5]\}$
mrmr	$0.03125\{4[4\beta_1^2(1-\beta_1)^2 + \beta_1^2(1-\beta_1) + \beta_1(1-\beta_1)^2] + [\beta_1^2 + (1-\beta_1)^2 + 2\beta_1(1-\beta_1) + 1]\}$
rrrr	$0.0625\{4[\beta_1^2(1-\beta_1)^2] + [\beta_1^2(1-\beta_1) + \beta_1(1-\beta_1)^2 + \beta_1(1-\beta_1) + 0.25]\}$
mrrr	$0.03125\{4[\beta_1^3(1-\beta_1) + \beta_1(1-\beta_1)^3 + 2\beta_1^2(1-\beta_1)^2 + \beta_1^2(1-\beta_1) + \beta_1(1-\beta_1)^2] + [\beta_1^2 + (1-\beta_1)^2 + 2\beta_1(1-\beta_1) + 1]\}$
mrrm	$0.03125\{4[\beta_1^3(1-\beta_1) + \beta_1(1-\beta_1)^3] + 2[\beta_1^2(1-\beta_1) + \beta_1(1-\beta_1)^2] + [\beta_1^2 + (1-\beta_1)^2 + 0.5]\}$

[a] Expressions for the isotactic and atactic sequences in terms of a site-control model have been derived elsewhere.[2b]

The most complicated expression ensues from the random model in that there are 64 possible sequences that must be considered, each with its own characteristic probability. The probability of insertion at site 1 with "correct" stereochemistry would be given by $W_i\beta_1$ (=A) whereas the other possibility at this site is given by $W_i(1-\beta_1)$ (=B). Assuming $\beta_2 = 0.5$, the corresponding probability for insertion at site 2 is $0.5W_a = 0.5(1 - W_i)$ (=C). The derivation for, e.g., the mrrr pentad using this model is outlined in Scheme 4, and the expressions for all pentads are summarized in Table 3.

Finally, similar condensations apply to the alternate model, except there are far fewer sequences that need to be considered (i.e., only 2, Scheme 5) and the pentad expressions are thus easy to derive (Table 4). This model can be extended to the more general case where $\beta_2 \neq 0.5$, and the relevant expressions for the pentad intensities are also summarized in Table 4.

Scheme 4

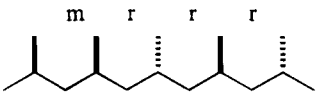

Site					Probability[a]		Site					Probability[a]	
1	1	1	1	1	A^3B^2	A^2B^3	2	2	2	2	2	C^5	C^5
1	1	1	1	2	A^3BC	AB^3C	2	2	2	2	1	BC^4	AC^4
1	1	1	2	1	A^2B^2C	A^2B^2C	2	2	2	1	2	AC^4	BC^4
1	1	2	1	1	A^3BC	AB^3C	2	2	1	2	2	BC^4	AC^4
1	2	1	1	1	A^2B^2C	A^2B^2C	2	1	2	2	2	AC^4	BC^4
2	1	1	1	1	A^2B^2C	A^2B^2C	1	2	2	2	2	AC^4	BC^4
1	1	1	2	2	A^2BC^2	AB^2C^2	2	2	2	1	1	ABC^3	ABC^3
1	1	2	1	2	A^3C^2	B^3C^2	2	2	1	2	1	B^2C^3	A^2C^3
1	2	1	1	2	A^2BC^2	AB^2C^2	2	1	2	2	1	ABC^3	ABC^3
1	2	1	2	1	AB^2C^2	A^2BC^2	2	1	2	1	2	A^2C^3	B^2C^3
1	1	2	2	1	A^2BC^2	AB^2C^2	2	2	1	1	2	ABC^3	ABC^3
1	2	2	1	1	A^2BC^2	AB^2C^2	2	1	1	2	2	ABC^3	ABC^3
2	1	1	1	2	A^2BC^2	AB^2C^2	1	2	2	2	1	ABC^3	ABC^3
2	1	1	2	1	AB^2C^2	A^2BC^2	1	2	2	1	2	A^2C^3	B^2C^3
2	1	2	1	1	A^2BC^2	AB^2C^2	1	2	1	2	2	ABC^3	ABC^3
2	2	1	1	1	AB^2C^2	A^2BC^2	1	1	2	2	2	A^2C^3	B^2C^3

mrrr = [normalization constant][symmetry factor][sum of probabilities]

= [1/64][2][sum of probabilities]

= [1/32][$A^3B^2 + A^2B^3 + 2A^3BC + 2AB^3C + 6A^2B^2C + 9A^2BC^2 + 9AB^2C^2 + A^3C^2 + B^3C^2 +$

$12ABC^3 + 4A^2C^3 + 4B^2C^3 + 5AC^4 + 5BC^4 + 2C^5$]

a. $A = W_i\beta_1$, $B = W_i(1-\beta_1)$ and $C = (1-W_i)(0.5)$

Table 3. Pentad Intensities for the Random Two-State Model[a]

pentad	probability[b]
mmmm	$[A^5 + B^5 + 5A^4C + 5B^4C + 10A^3C^2 + 10B^3C^2 + 10A^2C^3 + 10B^2C^3 + 5AC^4 + 5BC^4 + 2C^5]$
mmmr	$2.0[A^4B + AB^4 + A^4C + B^4C + 4A^3BC + 4AB^3C + 4A^3C^2 + 4B^3C^2 + 6A^2BC^2 + 6AB^2C^2 + 8ABC^3 + 6A^2C^3 + 6B^2C^3 + 5AC^4 + 5BC^4 + 2C^5]$
rmmr	$[A^3B^2 + A^2B^3 + 2A^3BC + 2AB^3C + 6A^2B^2C + 9A^2BC^2 + 9AB^2C^2 + A^3C^2 + B^3C^2 + 12ABC^3 + 4A^2C^3 + 4B^2C^3 + 5AC^4 + 5BC^4 + 2C^5]$
mmrr	[mmmr]
mrmm + rmrr	4.0[rmmr]
mrmr	2.0[rmmr]
rrrr	[rmmr]
mrrr	2.0[rmmr]
mrrm	0.5[mmmr]

[a] All expressions should be multiplied by a normalization constant of 1/64 = 0.015625; see Scheme 4. [b] $A = W_i\beta_1$, $B = W_i(1 - \beta_1)$, and $C = (1 - W_i)(0.5)$.

Model Comparison. A computer program was developed to test each of these models (models I–III) which used as input the experimental pentad distribution and which varied the parameters over a predetermined range of values (e.g., for the random model; $0.5 < \beta_1 < 1.0$ and $0.0 < W_i < 1.0$) so as to minimize the residual sum of squares (RSS) between the calculated and observed pentad distributions.

Scheme 5

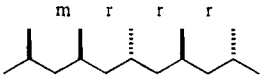

Site of Insertion					Probability of mrrr Pentad	
1	2	1	2	1	$\beta(1-\beta)2\cdot0.5^2$	$\beta^2(1-\beta)0.5^2$
2	1	2	1	2	$\beta^2 0.5^3$	$(1-\beta)^2 0.5^3$

mrrr = [normalization constant] [symmetry factor][sum of probabilities]

= [0.5][2][sum of probabilities]

= $0.25[\beta(1-\beta)^2 + \beta^2(1-\beta) + \beta^2 0.5 + (1-\beta)^2 0.5]$

Examples of the calculated (and experimental) distributions for each model along with the parameter values and the error as reflected in the RSS are summarized in Table 5.[11]

The alternate model did not satisfactorily account for the microstructure of elPP using the initial assumption of $\beta_2 = 0.5$; in order to provide a fit to the data equivalent to those of models I and II, it was necessary to relax this criterion and to make use of the more complicated expressions summarized in Table 4. It is also clear that both the block and random models fit the data with essentially equal precision in most cases.

Table 4. Pentad Intensities for the Alternate Model

pentad	probability[a]	pentad	probability[b]
mmmm	$0.5C^2[A^3 + B^3 + C(A^2 + B^2)]$	mmmm	$0.5[A^2C^2(A + C) + B^2D^2(B + D)]$
mmmr	$C^2[C(A^2 + B^2) + AB(A + B)]$	mmmr	$[A^2C^2(B + D) + B^2D^2(A + C)]$
rmmr	0.5[mmmr]	rmmr	$0.5[B^2C^2(A + D) + A^2D^2(B + C)]$
mmrr	$C^2[A^3 + B^3 + 2ABC]$	mmrr	$[CD(A^3 + B^3) + AB(C^3 + D^3)]$
mmrm + rrmr	$4ABC^2$	mmrm + rrmr	$4[ABCD]$
mrmr	0.5[mrmr + rrmr]	mrmr	$2[ABCD]$
rrrr	[mmmm]	rrrr	$0.5[A^2D^2(A + D) + B^2C^2(B + C)]$
mrrr	[mmmr]	rrrm	2[rmmr]
mrrm	0.5[mmmr]	mrrm	0.5[mmmr]

[a] $A = \beta_1$, $B = (1 - \beta_1)$, $C = \beta_2 = (1 - \beta_2) = 0.5$. [b] $A = \beta_1$, $B = (1 - \beta_1)$, $C = \beta_2$, $D = (1 - \beta_2)$.

Table 5. Comparison of Models for Pentad Intensities of Poly(propylene) Prepared Using Catalysts 2 and 4–6[a]

	2				**4**				**5**				**6**			
		model[b]				model[b]				model[b]				model[b]		
pentad	exp	I	II	III	exp	I	II	III	exp	I	II	III	exp	I	II	III
mmmm	0.359	0.361	0.354	0.354	0.370	0.369	0.378	0.376	0.297	0.299	0.297	0.299	0.528	0.524	0.528	0.528
mmmr	0.175	0.166	0.165	0.165	0.187	0.165	0.164	0.160	0.171	0.167	0.167	0.167	0.158	0.145	0.144	0.144
rmmr	0.026	0.024	0.023	0.023	0.030	0.022	0.021	0.025	0.048	0.029	0.029	0.028	0.021	0.011	0.011	0.011
mmrr	0.149	0.147	0.165	0.165	0.186	0.164	0.164	0.176	0.153	0.165	0.167	0.167	0.139	0.144	0.144	0.144
mrmm + rmrr	0.111	0.112	0.093	0.093	0.065	0.089	0.085	0.067	0.114	0.116	0.114	0.114	0.043	0.046	0.045	0.045
rmrm	0.043	0.048	0.046	0.046	0.018	0.044	0.042	0.034	0.061	0.057	0.057	0.057	0.022	0.023	0.022	0.022
rrrr	0.016	0.021	0.023	0.023	0.018	0.022	0.021	0.031	0.026	0.028	0.029	0.028	0.008	0.011	0.011	0.011
rrrm	0.050	0.051	0.046	0.046	0.032	0.044	0.042	0.049	0.043	0.057	0.057	0.057	0.017	0.023	0.022	0.022
mrrm	0.070	0.071	0.083	0.083	0.094	0.082	0.082	0.080	0.087	0.082	0.083	0.083	0.064	0.072	0.072	0.072
parameters[c,d]																
β_1		0.860	0.940	0.815		0.820	0.965	0.900		0.790	0.860	0.785		0.880	0.900	0.880
W_i		0.660	0.710	0.500		0.990	0.695	0.500		0.950	0.790	0.500		0.990	0.950	0.500
β_2		0.500	0.500	0.810		0.500	0.500	0.750		0.500	0.500	0.785		0.500	0.500	0.880
W_a		0.000	0.290	0.500		0.000	0.305	0.500		0.000	0.210	0.500		0.000	0.050	0.500
W_{sb}		0.340	*e*	*e*		0.010	*e*	*e*		0.050	*e*	*e*		0.010	*e*	*e*
RSS ($\times 10^3$)		0.15	0.96	0.96		2.58	2.40	1.79		0.80	0.82	0.82		0.43	0.42	0.42

[a] All polymerizations were conducted in toluene solution at 25 °C and with a propylene pressure of 15 psig. [b] For a description of models I–III, see the text. [c] For definition of the parameters, see text and Schemes 3–5. [d] The values recorded are those that minimized the errors; in most cases there are more solutions which fit the data with equal accuracy (see text). [e] W_{sb} is not defined for models II and III.

Somewhat surprisingly, the fit to the data (using either model I or II) was not routinely improved by relaxing the restriction on β_2.

Thus, from these examples, it is evident that the microstructure of elPP can be adequately described by either a model which invokes a block type structure or ones that do not! In other words, the observation that a consecutive insertion model does fit the data does not necessarily mean that elPP has the microstructure shown in structure I.

Another meaningful question that may be posed is whether the parameters summarized in Table 5 are uniquely determined. That is, are there other solutions for each model that fit the data with a certain degree of precision?

As a *conservative* estimate of the experimental error associated with the measurement of pentad intensities by NMR (±5% corresponding to a RSS of 0.0025), we obtained possible parameter values for both the block and random models that gave calculated distributions within this error.

As shown in Figure 1, this approach generates a family or contour of acceptable values for the parameters for which the "best" fit lies at the center of the contour. This feature is true of either model but it is clear from Figure 1 that the range of acceptable values is different for each.

The random model has a lower limit to β_1 but no upper limit (i.e., $\beta_1 \leq 1.0$) whereas the block model has the same lower limit for β_1 (as it must since $W_i = 1.0$ at this point) but also has an upper limit. For the example

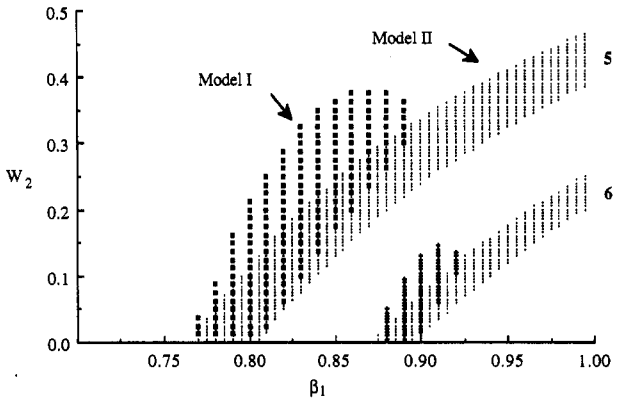

Figure 1. Acceptable solutions (RSS ≤ 0.0025) using models I and II for the microstructure of PP prepared using catalysts **5** and **6** (25 °C, 15 psig). The weight fraction of insertion from site 2 ($W_2 = W_a + 0.5W_{sb}$ for model I and $W_2 = W_a$ for model II) is plotted vs the stereoselectivity of insertion at site 1 (β_1).

shown, β_1 must be ≤0.90 regardless of the relative frequencies of insertion at sites 1 and 2.

This exercise demonstrates the danger of trying to deduce (chemically) meaningful parameter estimates (for *either* model) solely on the basis of the observed pentad distribution. More importantly, it demonstrates that discrimination between, e.g., the block and random models requires an independent estimate of one of the parameters common to both.

Discussion. The foregoing analysis has demonstrated that the microstructure of elPP can be satisfactorily described by either the block or random models

Scheme 6

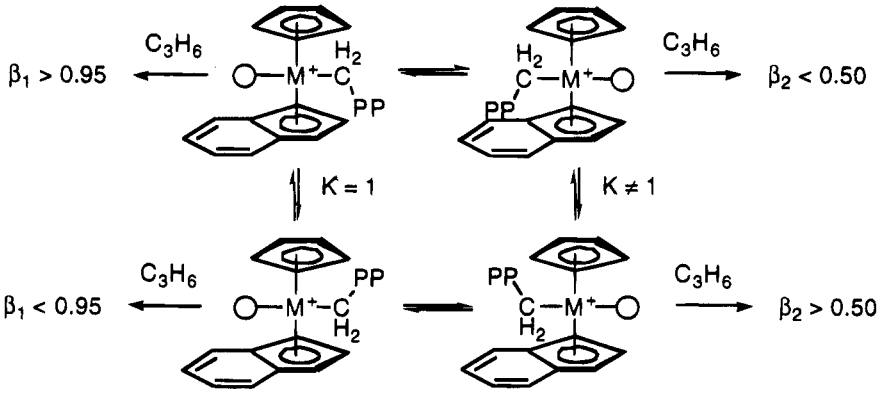

but not by the alternate model if it is assumed that insertions at site 2 are stereorandom (i.e., $\beta_2 = 0.5$).

One may question the validity of this assumption; the orientation of the polymer chain may exert an indirect influence on the stereochemistry of insertion at site 2 as shown in Scheme 6. This effect has been alluded to in several theoretical studies on olefin insertion.[12] In the present case, the preferred orientation of the polymer chain is expected to be the one shown at the lower right corner of this scheme, which should favor propylene insertion at site 2 via the *same* enantioface as isospecific insertions at site 1. Indeed, if the restriction on β_2 is relaxed, the alternate model predicts this preference and acceptable pentad distributions can be obtained (Table 5).

By the same token, it is not clear what is a reasonable estimate for β_1, the stereoselectivity of insertion at site 1. If the orientation of the polymer chain is important, one would expect diminished stereoselectivity at site 1 (compared with analogous insertions at a sterically equivalent site using an isospecific, C_2 symmetric catalyst) since the chain is able to adopt two, roughly isoenergetic conformations (Scheme 6) and insertion should occur with different stereochemical outcomes.

A brief perusal of the results obtained using model III (Table 5) reveals that the best solution usually has $\beta_1 \sim \beta_2$. This is a nonsensical result and suggests that in the absence of other estimates of these parameters, this model, although attractive from a fundamental viewpoint, cannot reliably be used.

If we assume that the stereoselectivity of insertion at site 1 is similar to that observed using an isospecific metallocene, it is possible to compare the block and random models in a meaningful fashion. For example, the stereoselectivity for insertion at site 1 in catalyst **5** should be similar to that observed using the C_2 symmetric catalyst *rac*-$Me_2Si(\eta^5$-indenyl$)_2ZrCl_2$.[13] Under comparable conditions to those studied here,[14] the isotactic polymer produced has mmmm = 0.93, which corresponds to a value of $\beta_1 = 0.985$. While this value is compatible with the random model, it is clearly not in agreement with the predictions of the block (or even the alternate[15]) model.

Of relevance to this issue are some observations concerning the low-temperature polymerization behavior of catalysts **1** and **2**. Below −20 °C, the former catalyst produces atactic polymer whereas the latter produces isotactic material.[3,4]

As shown in Scheme 6, this makes some sense; the preferred location for the polymer chain (or aluminoxane counterion) in the latter case is expected to preferentially expose the isospecific site to monomer coordination

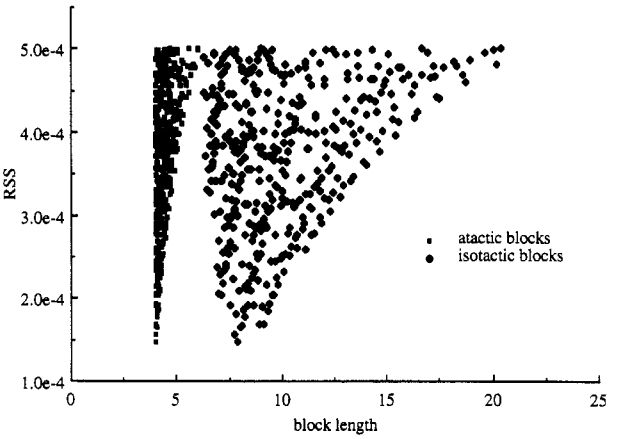

Figure 2. Average atactic and isotactic block lengths calculated from solutions to model I (RSS ≤ 0.0005) for PP prepared using catalyst **2** (25 °C, 15 psig). For the calculation of the block length, see ref 16.

and insertion whereas the opposite is true for catalyst **1**. The value of $\beta_1 = 0.95$ measured for this catalyst at this temperature probably represents a *lower* bound for the stereoselectivity for insertion at site 1. Based on the observed microstructure at 25 °C (Table 1), the block model cannot account for this distribution unless a lower value for β_1 is assumed.

A more meaningful approach for the present purpose is to assume that the block model is correct—i.e., the structure of elPP is correctly represented by structure I. If, for example, the atactic blocks are long, as would be required based on the mechanism proposed (i.e., only occasional chain isomerization during propagation), then W_{sb}, the amount of polymer contained within the sequence boundary, should be small compared to W_a (and W_i). A brief perusal of some of the parameter estimates contained within Table 5 reveals that this is most often not the case.

A second related question that can be posed is, what is the average block length? As we did not assume a fixed block length in our derivation of this model (other than it being >4 monomer units), this type of analysis is possible. The results of this analysis are depicted in Figure 2 in which the average block length for insertions at sites 1 and 2 was calculated[16] for all possible solutions of the block model that fit the data obtained using catalyst **2** (Table 5) with RSS ≤ 0.0005.[17] This figure reveals that the vast majority of solutions predict the average block length is quite short and the best solutions indicate that the average block length for insertions at site 2 is little more than 4 monomer units long. A much wider range of average block lengths for

Scheme 7

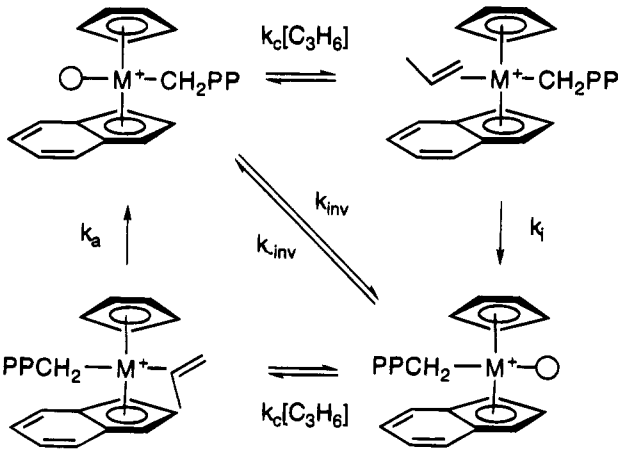

insertion at site 1 is tolerated but the best solutions predict a value close to 10 monomer units. Thus, if the block model is valid, this finding implies that chain isomerization is occurring much more frequently than originally envisaged and that the amorphous domains[5] must contain large amounts of short isotactic and atactic sequences. An isotactic block of 10 monomer units is too short to crystallize; the minimum isotactic sequence length for crystallization in elPP has been estimated at between 11 and 15 monomer units.[18] Any of these models could be employed to determine the sequence length distribution in these polymers, and it would be useful to explore the relationship between these predictions and the physical properties of elPP (e.g., crystallinity) scaled to molecular weight; qualitatively, the low crystallinity observed for these polymers[4] tends to indicate that only a small fraction of the isotactic sequences present actually (co)crystallize to generate the elastomeric network.

Finally, we note that the stereoselectivity of insertion was surprisingly sensitive to changes in monomer concentration using catalysts **2**–**6**;[4] higher monomer concentrations led to decrease in stereoregularity of the polymer produced. With reference to Scheme 7, this can be readily explained. Fundamentally, there should be a tendency toward site alternation in all polymerizations involving metallocene catalysts, in that the migratory insertion process effects the interchange of coordination sites for monomer and polymer chain. However, the tendency toward alternation should increase as the rate of propagation increases relative to the rate of chain isomerization. Since the rate of the former process is dependent on monomer concentration whereas the rate of the latter is probably not, one expects increased alternation at higher monomer concentrations. In the present case, our models indicate that site 1 is the more reactive or available site for monomer coordination (i.e., $W_1 > 0.5$), which implies that chain isomerization following insertion at site 1 is more rapid than monomer coordination and insertion at site 2. An increase in monomer concentration should make the latter process more competitive and would result in a decrease in the stereoregularity of the polymer as observed. This type of propagation scheme also seems to account for the effects of monomer concentration described by others using isospecific or syndiospecific catalysts.[19]

Conclusions

The microstructure of elPP can be successfully described by a number of statistical models including those that do not rely on consecutive insertions from a given lateral coordination site as originally proposed.[3,7]

From a chemical perspective, none of the these models have meaningful predictive value, in that there are a large number of solutions that are in excellent agreement with the measured pentad distributions even if simplifying assumptions are made.

Quite clearly, our understanding of polymer chain dynamics in these catalyst systems leaves much to be desired; fundamental studies along these lines may help to resolve mechanistic issues such as those involved in the formation of elPP.

Finally, it seems that the actual microstructure of elPP cannot be unambiguously assigned on the basis of statistical models for the pentad distribution. While fundamental considerations suggest that elPP may not have the idealized block microstructure originally suggested, measurement of the pentad (or higher) distributions of these polymers is unlikely to be informative and independent, unambiguous measurements will be required to resolve this issue.

Acknowledgment. The authors wish to thank the Natural Sciences and Engineering Research Council for financial support of this work. The assistance of Mr. J. R. Gauthier in the development of the computer code required for the modeling of the pentad intensities is gratefully acknowledged. Copies of this program are commercially available from the authors on request.

References and Notes

(1) Current address: W. R. Grace Co., Washington Research Centre, 7379 Route 32, Columbia, MD 02144.
(2) (a) For general treatment of the various models, see: Bovey, F. A. *High Resolution NMR of Macromolecules*, Academic Press: New York, 1972. See also: (b) Fueno, T.; Sheldon, R. A.; Furukawa, J. *J. Polym. Sci.* **1965**, *A3*, 1279. (c) Lowry, G. G. *Markov Chains and Monte Carlo Calculations in Polymer Science*; Marcel Dekker: New York, 1970. (d) Zambelli, A.; Locatelli, P.; Sacchi, M. C.; Tritto, I. *Macromolecules* **1982**, *15*, 831 and references therein. (e) Inoue, Y.; Itabashi, Y.; Chujo, R.; Doi, Y. *Polymer* **1984**, *25*, 1641. (f) Cheng, H. N. In *Transition Metal Catalyzed Polymerizations: Ziegler–Natta and Metathesis Polymerizations*; Quirk, R. P., Hoff, R. E., Klingensmith, G. B., Tait, P. J. T., Goodall, B. L., Eds.; Cambridge University Press: Cambridge, 1988. (g) Paukkeri, R.; Vaananen, T.; Lehtinen, A. *Polymer* **1993**, *34*, 12. (h) van de Burg, M. W.; Chadwick, J. C.; Sudmeijer, O.; Tulleken, H. J. A. F. *Makromol. Chem., Theory Simul.* **1993**, *2*, 399.
(3) (a) Mallin, D. T.; Rausch, M. D.; Lin, G.-Y.; Dong, S.; Chien, J. C. W. *J. Am. Chem. Soc.* **1990**, *112*, 2030. (b) Chien, J. C. W.; Llinas, G. H.; Rausch, M. D.; Lin, G.-Y.; Winter, H. H. *Ibid.* **1991**, *113*, 8569. (c) Chien, J. C. W.; Llinas, G. H.; Rausch, M. D.; Lin, G.-Y.; Winter, H. H.; Atwood, J. L.; Bott, S. G. *J. Polym. Sci., Polym. Chem.* **1992**, *30*, 2601. (d) Llinas, G. H.; Day, R. O.; Rausch, M. D.; Chien, J. C. W. *Organometallics* **1993**, *12*, 1283.
(4) Gauthier, W. J.; Corrigan, J. F.; Taylor, N. J.; Collins, S. *Macromolecules* **1995**, *28*, 3771.
(5) (a) Lin, G.-Y.; Mallin, D. T.; Chien, J. C. W.; Winter, H. H. *Macromolecules* **1991**, *24*, 850. (b) Llinas, G. H.; Dong, S.-H.; Mallin, D. T.; Rausch, M. D.; Lin, G.-Y.; Winter, H. H.; Chien, J. C. W. *Ibid.* **1992**, *25*, 1242.
(6) (a) Coleman, B. D.; Fox, T. G. *J. Chem. Phys.* **1963**, *38*, 1065. (b) Coleman, B. D.; Fox, T. G. *J. Polym. Sci., Part A* **1963**, *1*, 3183.
(7) (a) Cheng, H. N.; Babu, G. N.; Newmark, R. A.; Chien, J. C. W. *Macromolecules* **1992**, *25*, 6980. (b) Babu, G. N.; Newmark, R. A.; Cheng, H. N.; Llinas, G. H.; Chien, J. C. W. *Ibid.* **1992**, *25*, 7400.
(8) Although shorter block lengths can be treated statistically, it seems unreasonable to do so given that a block of four monomer units is the shortest that can be determined experimentally by ^{13}C NMR spectroscopy.
(9) Grassi, A.; Zambelli, A.; Resconi, L.; Albizzatti, E.; Mazzochi, R. *Macromolecules* **1988**, *21*, 617 and references therein.

(10) Farina, M.; Di Silvestro, G.; Sozzani, P. *Macromolecules* **1993**, *26*, 946.
(11) Although not shown, the use of model I gave equivalent results to the consecutive model developed by Cheng et al.[7] to describe the microstructure of elPP prepared using catalyst **1**. Gauthier W. J. Ph.D. Thesis, University of Waterloo, 1994.
(12) See, inter alia: (a) Kawamura-Kuribayashi, H.; Koga, N.; Morokuma, K. *J. Am. Chem. Soc.* **1992**, *114*, 2359. (b) Castonguay, L. A.; Rappe, A. K. *Ibid.* **1992**, *114*, 5832. (c) Prosenc, M.-H.; Janiak, C.; Brintzinger, H. H. *Organometallics* **1992**, *11*, 4036 and references therein.
(13) Spaleck, W.; Antberg, M.; Dolle, V.; Klein, R.; Rohrmann, J.; Winter, A. *New J. Chem.* **1990**, *14*, 499.
(14) Spaleck, W.; Antberg, M.; Rohrmann, J.; Winter, A.; Bachmann, B.; Kiprof, P.; Behm, J.; Hermann, W. A. *Angew. Chem., Int. Ed. Engl.* **1992**, *31*, 1347.
(15) If perfect alternation is assumed (i.e., $W_i = W_a = 0.5$), the maximum value of β_1 (or β_2) is <0.90 for those solutions using model III with RSS $\leq$ 0.0025.
(16) The average block length arising from insertions at a given site using model I is related to the expression for the average isotactic run length in isotactic polypropylene which is $N_{iso} = 4 + 2(\text{mmmm})/(\text{mmmr})$. Here, however, one is considering the number of sequential insertions from, e.g., site 1 $\geq$5 monomer units which is given by the parameter W_i and is entirely analogous to the normalized intensity of a mmmm pentad. Since a given sequence of consecutive insertions from site 1 $\geq$5 monomer units will always start and end with a sequence boundary (neglecting chain end effects), the analogous expression for the average block length is given by $N_1 = 4 + 2(W_i/W_{sb})$. A similar expression pertains to those sequential insertions occurring at site 2 that are $\geq$5 monomer units.
(17) The microstructure for the polymer prepared using catalyst **2** was modeled, as this was one of the only examples where the fit of model I was much better than that of model II or III (Table 5).
(18) Collete, J. W.; Ovenall, D. W.; Buck, W. H.; Ferguson, R. C. *Macromolecules* **1989**, *22*, 3858.
(19) (a) Reiger, B.; Jany, G.; Fawzi, R.; Steimann, M. *Organometallics* **1994**, *13*, 647. (b) Ewen, J. A.; Jones, R. L.; Razavi, A.; Ferrara, J. D. *J. Am. Chem. Soc.* **1988**, *110*, 6255.

MA9461660